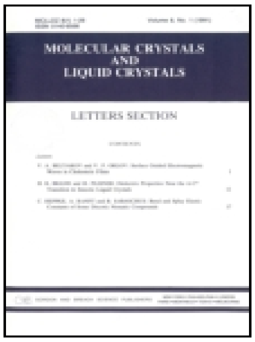

Taylor & Francis
Taylor & Francis Group

Molecular Crystals and Liquid Crystals

ISSN: 1542-1406 (Print) 1563-5287 (Online) Journal homepage: http://www.tandfonline.com/loi/gmcl20

Theoretical Study of Xanthenone and Phenothiazine Derivatives for Blue TADF Emitter

Dong Yuel Kwon, Geon Hyeong Lee & Young Sik Kim

To cite this article: Dong Yuel Kwon, Geon Hyeong Lee & Young Sik Kim (2015) Theoretical Study of Xanthenone and Phenothiazine Derivatives for Blue TADF Emitter, Molecular Crystals and Liquid Crystals, 620:1, 166-170, DOI: 10.1080/15421406.2015.1095443

To link to this article: http://dx.doi.org/10.1080/15421406.2015.1095443

Published online: 16 Dec 2015.

Submit your article to this journal

Article views: 26

View related articles

View Crossmark data

Full Terms & Conditions of access and use can be found at
http://www.tandfonline.com/action/journalInformation?journalCode=gmcl20

Download by: [East China University of Science and Technology] **Date:** 02 January 2016, At: 09:36

Mol. Cryst. Liq. Cryst., Vol. 620: pp. 166–170, 2015
Copyright © Taylor & Francis Group, LLC
ISSN: 1542-1406 print/1563-5287 online
DOI: 10.1080/15421406.2015.1095443

Downloaded by [East China University of Science and Technology] at 09:37 02 January 2016

Theoretical Study of Xanthenone and Phenothiazine Derivatives for Blue TADF Emitter

DONG YUEL KWON,[1] GEON HYEONG LEE,[1]
AND YOUNG SIK KIM[1,2,*]

[1]Department of Information Display, Hongik University, Seoul, Korea
[2]Department of Science, Hongik University, Seoul, Korea

Two novel thermally activated delayed fluorescence (TADF) materials (PTZ-XTN and 2PTZ-XTN), with phenothiazine (PTZ) as an electron donor and xanthenone derivatives (XTN) as electron acceptors, were designed and theoretically investigated as blue OLED emitters. We used density functional theory (DFT) and time dependent DFT (TD-DFT) calculations to determine the electron distribution of HOMO and LUMO and the energy of the lowest singlet (S_1) and the lowest triplet (T_1) excited states. The large dihedral angle between the electron donor and the electron acceptor imparted a small spatial overlap between HOMO and LUMO in all the materials. This charge separation of the HOMO and LUMO leads to a small energy gap between the S_1 state and T_1 state, thereby leading to TADF emission. Among the materials studied, PTZ-XTN has the most suitable properties for a blue TADF OLED emitter, even though 2PTZ-XTN has the smallest energy gap between the S_1 and T_1 states.

Keywords OLED; Thermally activated delayed fluorescence (TADF); DFT; TD-DFT

1. Introduction

In recent years, organic light-emitting diodes (OLEDs) have been extensively studied for application as next-generation flat-panel displays because of their high luminescence, low drive voltage, fast response, and abundant range of colors [1–3]. In small display fields, such as on mobile phones, OLED display panels are already being used and have been commercialized. However, the current choices of materials for fabricating OLEDs are not yet optimal. For example, fluorescent materials can emit light only via singlet excitons, which means that only a 25% maximum internal quantum efficiency (IQE) is obtained because carrier recombination produces singlet and triplet excitons in a 1:3 ratio through spin statics [4]. By contrast, phosphorescent materials based on noble heavy-metal phosphors can achieve high efficiency approaching nearly 100% of the IQE; consequently, phosphorescent materials and devices have been extensively studied in order to achieve a high efficiency for OLEDs. The heavy metals present in the complexes induce an intersystem crossing by strong spin-orbit coupling, which leads to a mixing of the singlet and triplet excited states [5, 6]. However, phosphorescent materials containing noble heavy metals,

---

[*]Address correspondence to Young Sik Kim, Department of Information Display, Hongik University, Seoul 121-791, Korea. E-mail: youngkim@hongik.ac.kr

Color versions of one or more of the figures in the article can be found online at www.tandfonline.com/gmcl.

Downloaded by [East China University of Science and Technology] at 09:37 02 January 2016

such as iridium, platinum, and osmium, are rather expensive and unsustainable. Thus, novel triplet harvesting methods for obtaining a high external quantum efficiency (EQE) are needed.

A new triplet harvesting method has recently been demonstrated that uses thermally activated up-conversion of triplet state (T_1) → singlet state (S_1) and provides thermally activated delayed fluorescence (TADF) with high EQE [7]. The energy of the S_1 level is considerably higher than the T_1 level, by $0.5 \sim 1.0$ eV, because of the electron exchange energy between these levels. The promotion of TADF requires a small energy gap between the S_1 state and the T_1 state (ΔE_{ST}) because the rate of $T_1 \rightarrow S_1$ reverse intersystem crossing (RISC) is inversely proportional to the exponential of ΔE_{ST} [8]. Therefore, an important factor in designing molecules with a small ΔE_{ST} is control of the spatial overlap between the highest occupied molecular orbital (HOMO) and the lowest unoccupied molecular orbital (LUMO) [9]. The value of ΔE_{ST} largely depends on the exchange interaction between electrons in molecular orbitals, implying electronic excitation; consequently, control of the spatial overlap between molecular orbitals is necessary. Thus, the molecular design of TADF emitters involves a careful choice of suitable donor and acceptor units. Adachi et al. previously reported a computational prediction for singlet and triplet transition energies of charge transfer compounds using the optimal Hartree-Fock (HF) exchange method [10].

In this study, we designed two TADF emitters (PTZ-XTN and 2PTZ-XTN) with phenothiazine (PTZ) as an electron donor and 9H-xanthen-9-one (XTN) as an electron acceptor, and investigated the electron distribution of HOMO and LUMO and the energy of the lowest singlet (S_1) and the lowest triplet (T_1) excited states. We compared these characteristics to those of a reference material 3-(9,9-dimethylacridin-10(9H)-yl)-9H-xanthen-9-one (ACR-XTN) [11].

2. Computational Details

To gain insight into the factors responsible for the absorption energy and the electron populations of molecular orbitals, we performed density functional theory (DFT) and time dependent DFT (TD-DFT) calculations on the ground state using a dependence on charge transfer (CT) amounts from donor to acceptor for the optimal Hartree-Fock (HF) percentage in the exchange-correlation of TD-DFT. The geometries in the gas phase were optimized by the DFT method by using the B3LYP exchange-correlation function with the 6-31G(d) basis set in the Gaussian 09 program package [12]. The possible isomers of the materials were also calculated using DFT. The present conformation was the lowest energy conformation, which is the optimal molecular structure of the materials in the gas phase. The electronic populations of the highest occupied molecular orbital (HOMO) and the lowest unoccupied molecular orbital (LUMO) were calculated to show the position of electron populations according to the calculated molecular orbital energy diagram. Vertical absorption energies [$E_{VA}(S_1)$] were calculated using TD-DFT with the BLYP, MPW1B95, BMK, M062X, and M06HF functionals with 6-31G(d) basis sets. To obtain an optimal HF% (OHF), we performed using the Multiwfn program [13] to analyze the orbital composition to determine the CT amount (q) value from donor to acceptor. We calculated $E_{VA}(S_1,\mathrm{OHF})$ from the relationship with OHF and q (OHF = 42q), and the zero−zero transition energies ($E_{0\text{-}0}$) of S_1 [$E_{0\text{-}0}(S_1)$] was obtained using the common gap of 0.24 eV between $E_{VA}(S_1,\mathrm{OHF})$ and $E_{0\text{-}0}(S_1)$, and $E_{0\text{-}0}(^3\mathrm{CT})$, $E_{0\text{-}0}(^3\mathrm{LE})$ and $E_{VE}(S_1)$ were obtained using the proven methods of Adachi et al [10].

Downloaded by [East China University of Science and Technology] at 09:37 02 January 2016

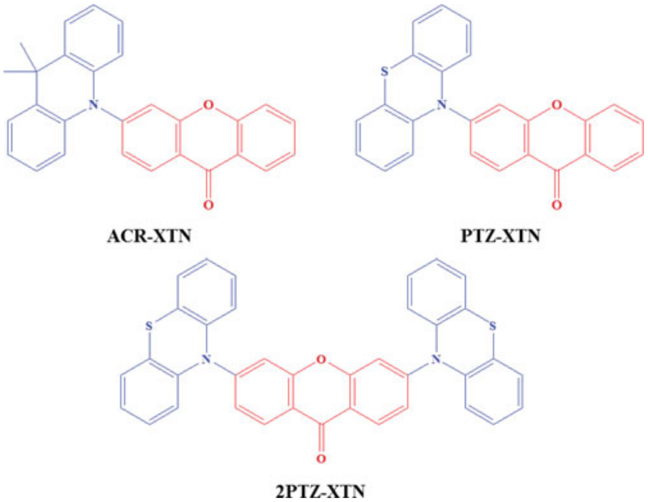

Figure 1. Molecular structure of ACR-XTN, PTZ-XTN, and 2PTZ-XTN (red color: acceptor, blue color: donor).

3. Results and Discussion

The schematic molecular structures of the materials considered in this study are shown in Fig. 1. ACR-XTN is the reference material, where 9,10-dihydro-9,9-dimethylacridine (ACR) serves as an electron donor and 9H-xanthen-9-one (XTN) as an electron acceptor [11]. ACR-XTN has a small ΔE_{ST} and a small spatial overlap between HOMO and LUMO, so it would show the TADF phenomenon but its emission color was green (490 nm). Therefore, we designed PTZ-XTN and 2PTZ-XTN to fabricate a blue TADF OLED emitter by the replacement of ACR with phenothiazine (PTZ) as an electron donor, as PTZ has a lower HOMO energy level than ACR. A study of the dihedral angle between the donor moiety and the acceptor moiety revealed that an increase in the dihedral angle between the donor moiety and the acceptor moiety was accompanied by a decrease in π-conjugation between the two moieties, which caused the triplet energy to increase and the spatial overlap between HOMO and LUMO to be small [14, 15]. The dihedral angles between the donor moiety and the acceptor moiety of PTZ-XTN, 2PTZ-XTN, and ACR-XTN were 81.67°, 81.47°, and 88.93°, respectively. These angles are sufficiently large to generate a small spatial overlap between HOMO and LUMO, so we expected that all three materials would have a small ΔE_{ST} and show the TADF phenomenon.

DFT calculations were performed at a B3LYP/6-31G(d) level to optimize the geometry of these materials in order to obtain their molecular orbitals and electronic structures. The electron distribution of the HOMO and the LUMO for PTZ-XTN, 2PTZ-XTN, and ACR-XTN are shown in Fig. 2. The electron population of all three materials show similar patterns in which the HOMO is mainly delocalized on the electron donor (ACR, and PTZ), demonstrating that both ACR and PTZ have strong electron donating abilities. The LUMO is mainly delocalized on the electron acceptor (XTN), demonstrating that XTN has strong electron withdrawing abilities. Consequently, as we expected, all three materials have a small spatial overlap between the HOMO and the LUMO.

The calculated CT amount (q), OHF%, oscillator strength, S_1 state energies, and T_1 state energies of each material, according to the TD-DFT calculation, are shown in Table 1. The

Downloaded by [East China University of Science and Technology] at 09:37 02 January 2016

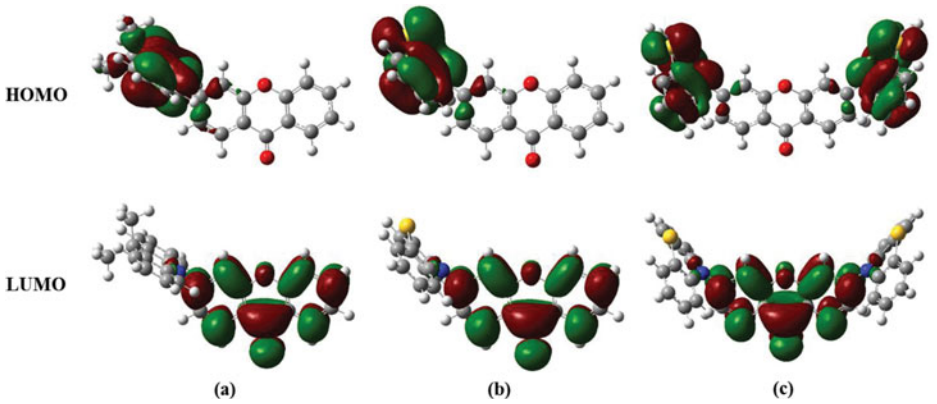

Figure 2. Electron distribution of HOMO and LUMO: (a) ACR-XTN, (b) PTZ-XTN, and (c) 2PTZ-XTN.

relatively large dihedral angle and the large CT amount from donor to acceptor generated a small spatial overlap between HOMO and LUMO in all three materials, so we expected that each would have a small ΔE_{ST}. The calculated ΔE_{ST} of ACR-XTN was 0.01 eV, which was similar to the experimental data (0.06 eV) [11], and the calculated ΔE_{ST} of PTZ-XTN and 2PTZ-XTN were 0.098 eV and 0.009 eV, respectively, which were small enough for RISC. A study of the material structure type revealed that the photoluminescence quantum yield (PLQY) was higher for a D-A-D type structure than for a D-A type structure when using the same electron donor and electron acceptor because the ΔE_{ST} was smaller for the D-A-D type structure than for the D-A type structure [16]. In terms of D-A type structure material, the dihedral angle was larger for ACR-XTN than for PTZ-XTN, which means that the steric hindrances were also larger for ACR-XTN than for PTZ-XTN. However, this difference was not significant and both materials had a sufficiently small ΔE_{ST} values. As previously mentioned, $E_{VE}(S_1)$ of ACR-XTN (2.52 eV) was too close to a green color, but that of PTZ-XTN (2.67 eV) was suitable for emission of a blue color. PTZ-XTN was also more suitable than 2-PTZ-XTN as a blue TADF OLED emitter, even though 2PTZ-XTN had the smallest ΔE_{ST} because of its $E_{VE}(S_1)$ value.

Table 1. Calculated energies and dihedral angle of the materials

	ACR-XTN	PTZ-XTN	2PTZ-XTN
Optimal HF%	36.9825	37.7230	36.1614
Dihedral angle (°)	88.93	81.67	81.47
$E_{VA}(S_1)$ (eV)	3.0038	3.1546	2.9671
$E_{0\text{-}0}(S_1)$ (eV)	2.7638	2.9146	2.7271
$E_{0\text{-}0}(^3CT)$ (eV)	2.7527	2.9054	2.7185
$E_{0\text{-}0}(^3LE)$ (eV)	2.7646	2.8166	2.7584
$E_{VE}(S_1)$ (eV, nm)	2.5238(491.3)	2.6746(463.6)	2.4871(498.6)
ΔE_{ST} (eV)	0.0111	0.0980	0.0086

4. Conclusions

We designed and investigated two XTN-based TADF materials using DFT and TD-DFT calculations and compared them to a reference TADF material, ACR-XTN. All three materials showed a small spatial overlap between the HOMO and LUMO because each donor and acceptor had strong donating and withdrawing abilities, and the TADF phenomenon could occur in all of them. As expected, all three materials had ΔE_{ST} values that were sufficiently small for showing the TADF phenomenon. However, the $E_{VE}(S_1)$ values of ACR-XTN and 2PTZ-XTN are too small for blue color emission, so we suggest PTZ-XTN as a good candidate for use as a blue TADF OLED emitter.

Acknowledgment

This research was supported by the Basic Science Research Program through the National Research Foundation of Korea (NRF) funded by the Ministry of Education, Science and Technology (2010-0021668).

References

[1] (a) Tang, C. W., and Vanslyke, S. A., (1987) *Appl. Phys. Lett.*, *51*, 913 (b) Adachi, C., Tsutsui, T., and Saito, S., (1989) *J. Appl. Phys.*, *55*, 813.

[2] Baldo, M. A., Lamansky, S., Burrows, P. E., Tompson, M. E., and Forrest, S. R., (1999) *Appl. Phys. Lett.*, *75*, 4.

[3] Baldo, M. A., Thompson, M. E., and Forrest, S. R., (2000) *Nature.*, *403*, 750.

[4] (a) Huang, C. W., Peng, K. Y., Liu, C. Y., Jen, T. H., Yang, N. J., and Chen, S. A., (2008) *Adv. Mater.*, *20*, 3709 (b) Zhang, Y., Lai, S. L., Tong, Q. X., Lo, M. F., Ng, T. W., Chan, M. Y., Wen, Z. C., He, J., Jeff, K. S., Tang, X. L., Liu, W. M., Ko, C. C., Wang, P. F., and Lee, C. S., (2012) *Chem. Mater.*, *24*, 61.

[5] (a) Baldo, M. A., O'Brien, D. F., You, Y., Shoustikov, A., Sibley, S., Thompson, M. E., and Forrest, S. R., (1998) *Nature.*, *395*, 151 (b) Adachi, C., Baldo, M. A., Thompson, M. E., and Forrest, S. R. J., (2001) *Appl. Phys.*, *90*, 5048.

[6] Ham, H. W., Jung, K. Y., and Kim, Y. S., (2010) *Thin Solid Film.*, *518*, 6199 (b) Park, S. W., Ham, H. W., and Kim, Y. S., (2012) *J. Nanosci. Nanotechnol.*, *12*, 3369.

[7] (a) Kondakov, D. Y., Pawlik, T. D., Hatwar, T. K., and Spindler, J. P., (2009) *J. Appl. Phys.*, *106*, 124510 (b) Endo, A., Sato, K., Yoshimura, K., Kai, T., Kawada, A., Miyazak, H., and Adachi, C., (2011) *Appl. Phys. Lett.*, *98*, 083302 (c) Goushi, K., Yoshida, K., Sato, K., and Adachi, C., (2012) *Nat. photonics.*, *6*, 253.

[8] Berberan-Santos, M. N., and Garcia, J. M. M., (1996) *J. Am. Chem. Soc.*, *118*, 9391.

[9] Lee, J., Shizu, K., Tanaka, H., Nomura, H., Yasudaabc, T., and Adachi, C., *J. Mater. Chem.*, (2013) *1*, 4599.

[10] Huang, S., Zhang, Q., Shiota, Y., Nakagawa, T., Kuwabara, K., Yoshizawa, K., and Adachi, C., (2013) *J. Chem. Theory Comput.*, *9*, 3872.

[11] Nakanotani, H., Higuchi, T., Furukawa, T., Masui, K., Morimoto, K., Numata, M., Tanaka, H., Sagara, Y., Yasuda, T., and Adachi, C., (2014) *Nat. Commun.*, *5*, 4016.

[12] (a) Lee, C., Yang, W., and Parr, R. G., (1988) *Phys. Rev. B.*, *37*, 785 (b) Miehlich, B., Savin, A., Stoll, H., and Preuss, H., (1989) *Chem. Phys. Lett.*, *157*, 200 (c) Becke, A. D., (1988) *Phys. Rev. A.*, *38*, 3098 (d) Becke, A. D., (1993) *J. Chem. Phys.*, *98*, 5648.

[13] Lu, T., and Chen, F. W., (2012) *J. Comput. Chem.*, *33*, 580.

[14] Tao, Y., Yang, C., and Qin, J., (2011) *Chem. Soc. Rev.*, *40*, 2943.

[15] Lee, S. Y., Yasuda, T., Yang, Y. S., Zhang, Q., and Adachi, C., (2014) *Angew. Chem.*, *126*, 6520.

[16] Lee, J., Shizu, K., Tanaka, H., Nomura, H., Yasuda, T., and Adachi, C., (2013) *J. Mater. Chem. C.*, *1*, 4599.

Downloaded by [East China University of Science and Technology] at 09:37 02 January 2016